Adsorption (2010) 16: 531–539
DOI 10.1007/s10450-010-9258-6

Characterization of the diffusion path in micro- and meso-porous materials from ZLC analysis

Qinglin Huang · Mladen Eić · Huining Xiao · Serge Kaliaguine

Published online: 5 August 2010
© Springer Science+Business Media, LLC 2010

Abstract It has been demonstrated that the main diffusion paths of micro- and meso-porous UL-zeolites could be characterized from the Zero Length Column (ZLC) desorption curves with an appropriate theoretical analysis (Malekian et al., in Ind. Eng. Chem. Res. 46:5067, 2007). The present work extends this method to study the ZLC desorption data of *n*-heptane/cumene/mesitylene in three mesoporous SBA-15 samples, 1-methylnaphthalene in MCM-48, cumene in SBA-16 and toluene/cumene in a microporous one-dimensional boron SSZ-42. The investigation results revealed that the structure of SBA-15, MCM-48 and SBA-16 behaved approximately as three-dimensional (isotropic) diffusion system, while SSZ-42 behaved as one-dimensional (anisotropic) diffusion systems. The diffusion path did not change within the measured temperature range, and by using different sorbate molecules. This work confirmed that this effective and relatively inexpensive method can be used as an additional tool for the characterization of porous materials.

Keywords Micro- and meso-porous material · Diffusion path, ZLC technique

1 Introduction

Microporous materials of three-dimensional structure (e.g., zeolites A, X, Y and carbon molecular sieve) or one-dimensional structure (e.g., $AlPO_4$-5, SAPO-5, silicalite, mordenite and ZSM-12) are widely used as adsorbents and catalysts in the petrochemical and hydrocarbon processing industry. Investigation of one-dimensional microporous materials as hydrocarbon trapping media for controlling vehicle cold start emission has also been reported (Iliyas et al. 2007; Sarshar et al. 2009). As molecules diffuse in microporous materials, they exhibit the corresponding one-/three-dimensional diffusion patterns. Such diffusion patterns have to be properly taken into account in the diffusion model used, to avoid significant errors that can be made in the calculations of diffusion parameters.

Since the discovery of ordered mesoporous silicas such as M41-S by Mobil Corporation scientists (Kresge et al. 1992) and SBA-n by Stucky and coworkers (Zhao et al. 1998), mesoporous materials have attracted great research interest in the field of catalysis (Trong-On et al. 2003), separation science (Vinh-Thang et al. 2005a) and drug delivery (Doadrio et al. 2006). Mesoporous materials have regular two-/three-dimensional distribution of mesopores with size ranging from 2 to 30 nm, allowing the penetration of large molecules. They were investigated for the use of light hydrocarbon adsorption separation and volatile organic component removal (Newalkar et al. 2002; Serrano et al. 2004). Metal substituted mesoporous materials were prepared to exploit their potential application as catalysts and catalyst supports (Rioux et al. 2005; Huang et al. 2008). Moreover, modification or functionalization of mesoporous surface via bonding of organic groups or polymers was carried out and investigated for controlled drug delivery system (Doadrio et al. 2006), liquid chromatography (Zhao et al. 2002), heavy metal removal (Liu et al. 2000), and carbon dioxide adsorption (Xu et al. 2003). In all of these applications, diffusion of sorbate molecules in the mesoporous materials can be the rate controlling step of overall transport process. There-

Q. Huang · M. Eić (✉) · H. Xiao
Department of Chemical Engineering, University of New Brunswick, Fredericton, NB, E3B 5A3, Canada
e-mail: meic@unb.ca

S. Kaliaguine
Department of Chemical Engineering, Laval University, Québec, G1K 7P4, Canada

fore, understanding diffusion pattern in these materials is of a considerable importance.

Ruthven and coworkers (Cavalcante et al. 1997) first proposed a method to characterize the diffusion patterns of microporous zeolites from Zero-Length-Column (ZLC) desorption analysis. In their study, they were able to distinguish the diffusion patterns in erionite (three-dimensional channel structure) and offretite (one-dimensional channel structure) using the proposed method. Recently, the same method has been successfully applied to assess the diffusion patterns involving micro-mesoporous and microporous materials, e.g., UL-ZSM5, ZSM-12 and ZSM-5 (Malekian et al. 2007). The aim of this work is to extend this method to characterize the diffusion pattern in mesoporous silicas SBA-15, SBA-16 and MCM-48, as well as a microporous boron SSZ-42, where similar analysis has not been reported in the literature yet.

2 Theory

The ZLC desorption technique was introduced by Eić and Ruthven (1988). For a linear equilibrium system with uniform spherical particles (three-dimensional channel system), the normalized effluent gas concentration (c/c_0) is given by:

$$\frac{c}{c_0} = 2L \sum_{n=1}^{\infty} \frac{\exp(-\beta_n^2 D_{\text{eff}} t/R_p^2)}{[\beta_n^2 + L(L-1)]} \tag{1}$$

where R is particle radius, D_{eff} is effective diffusivity and β_n are eigen-values given by the roots of the auxiliary equation:

$$\beta_n \cot \beta_n + L - 1 = 0 \tag{2}$$

and

$$L = \frac{F R_p^2}{3 K V_s D_{\text{eff}}} \tag{3}$$

where F is purge flow rate, V_s is adsorbent volume and K is Henry's law constant.

The corresponding full expression for slab-geometry, which corresponds to one-dimensional model, is presented as follows:

$$\frac{c}{c_0} = 2L \sum_{n=1}^{\infty} \frac{\exp(-\beta_n^2 D_{\text{eff}} t/l^2)}{[\beta_n^2 + L(L+1)]} \tag{4}$$

where β_n are eigenvalues given by the roots of the equation:

$$\beta_n \tan \beta_n - L = 0. \tag{5}$$

Effective diffusion time constants (D_{eff}/R_p^2) or (D_{eff}/l^2) and L value can be extracted by fitting the full time solution models, i.e., (1) and (2) or (4) and (5), with the experimental ZLC data.

To investigate diffusion pathways in porous materials a simple method based on an approximate solution of (1) and (4) was proposed by Ruthven and coworkers (Brandani and Ruthven 1996; Cavalcante et al. 1997). For a three-dimensional case the normalized effluent gas concentration (c/c_0) can be approximated as:

$$\frac{c}{c_0} = \frac{1}{L}\left[\sqrt{\frac{R_p^2}{\pi D_{\text{eff}} t}} - 1\right] \tag{6}$$

and for one-dimensional case:

$$\frac{c}{c_0} = \frac{1}{L}\left[\sqrt{\frac{l^2}{\pi D_{\text{eff}} t}}\right]. \tag{7}$$

Equations (6) and (7) are the model equations that are proposed to be used for diffusion pattern analysis. They are valid in the concentration range $c/c_0 < 0.2$ and $L > 10$ (L is extracted from full time solution method) (Cavalcante et al. 1997). For a three-dimensional diffusion path, a plot of c/c_0 versus $1/\sqrt{t}$ should yield an intercept $(-1/L)$, whereas, for one-dimensional diffusion path, the line should pass through the origin (zero). The shortcoming of the method is that for the large L values, the intercept becomes too small to easily distinguish between the zero and non-zero intercepts. However, the consistency of these models can be verified by first calculating the diffusion time constant from the slope of such a plot, followed by further cross-checking with the result obtained from the full time solution model.

3 Experimental

3.1 Materials

Three SBA-15 samples designated as SBA-15-1, SBA-15-2 and SBA-15-3, one SBA-16 sample and one boron SSZ-42 microporous sample were synthesized at Laval University. A detailed account of the synthesis procedures has been reported by Vinh-Thang et al. (2005b), Gobin et al. (2007) and Sarshar et al. (2009), respectively. The MCM-48 sample was prepared referring to the procedure described elsewhere (Huang et al. 2008). Important structural properties and pore volumes of the synthesized materials are summarized in Table 1.

3.2 ZLC measurements

Prior to measurement, 1–2 mg sample, which was placed between two sintered discs in the ZLC column, was activated overnight at 270 °C by purging with small flow of helium (∼10 cm^3/min). The sample was then fully equilibrated

Table 1 Textural properties of various samples

Sample	Heating time (day)	Synthesis temp. (°C)	S_{BET} (m^2/g)	Total pore volume (cm^3/g)	Micropore volume (cm^3/g)[a]	Mesopore volume (cm^3/g)	Mesopore diameter (nm)[b]
SBA-15-1	1	60	750	0.58	0.12	0.46	5.5
SBA-15-2	1	80	860	0.85	0.10	0.75	7.1
SBA-15-3	5	80	920	1.11	0.06	1.05	7.8
SBA-16	1	45	370	0.23	0.07	0.16	7.8
MCM-48	2	120	869	1.05	–	–	3.0
SSZ-42	17	150	495	–	0.19	–	–

[a]The micropore volume of SSZ-42 sample was determined by *t*-plot method, while those of SBA-15 and SBA-16 samples were determined by α_s-plot method

[b]Mesopore diameter was estimated using modified BJH method from nitrogen adsorption isotherm data at 77 K (Vinh-Thang et al. 2005b)

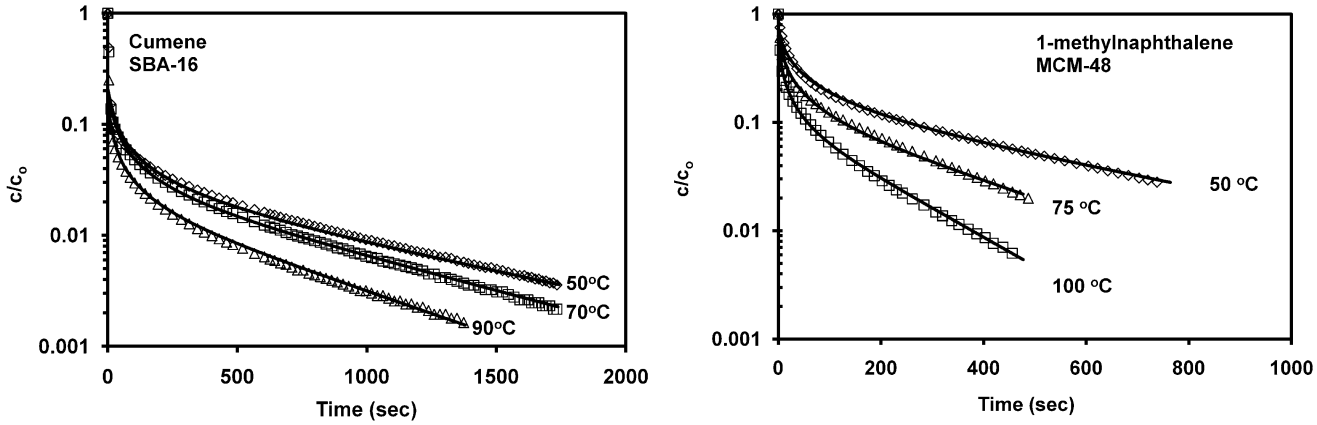

Fig. 1 Experimental (*symbols*) and theoretical (*solid lines*) ZLC curves for cumene in SBA-16 and 1-methylnaphthalene in MCM-48 at different temperatures

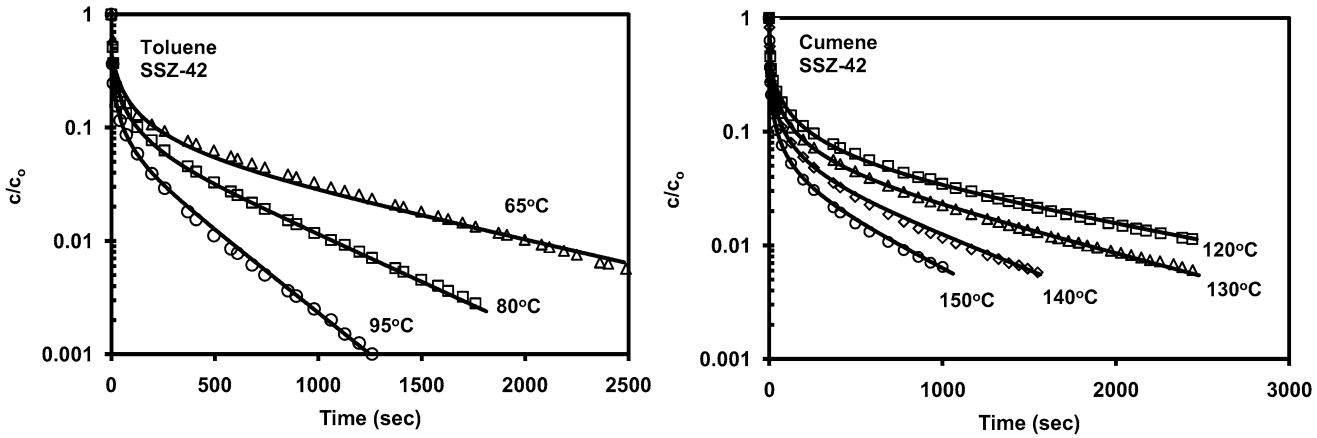

Fig. 2 Experimental (*symbols*) and theoretical (*solid lines*) ZLC curves of toluene and cumene in SSZ-42 sample

with sorbate diluted in a helium flow. The sorbate concentration was maintained low enough (e.g., 0.005–0.01 Torr partial pressure) to ensure that the measurements were carried out within the linear range of equilibrium isotherm, as required by the ZLC theory. The desorption measurement was performed by purging with pure helium at a flow rate high enough to maintain a very low sorbate concentration at the external surface of the particles, thus minimizing external heat and mass transfer resistance. Essentially the same diffusion parameters were extracted from the experimental

Table 2 Summary of parameters from the ZLC analysis of toluene and cumene in SSZ-42 sample based on (A) one-dimensional model and (B) three-dimensional model

A

Sorbate	Sorbent	T (°C)	Diffusion pattern analysis			Full time analysis			Relative difference of D_{eff}/l^2, ε (%)[a]
			Slope	D_{eff}/l^2 (s^{-1})	R^2-value	L	D_{eff}/l^2 (s^{-1})	R^2-value	
Cumene	SSZ-42	120	1.517	4.79×10^{-4}	0.9817	17	4.70×10^{-4}	0.9901	1.9
		130	1.194	6.90×10^{-4}	0.9819	18	6.33×10^{-4}	0.9910	9.0
		140	0.922	1.04×10^{-4}	0.9861	19	9.73×10^{-4}	0.9907	6.7
		150	0.658	1.18×10^{-3}	0.9930	25	1.17×10^{-3}	0.9925	0.4
Toluene	SSZ-42	65	1.444	5.97×10^{-4}	0.9893	16	5.59×10^{-4}	0.9936	6.8
		80	1.113	1.14×10^{-3}	0.9943	15	1.05×10^{-3}	0.9932	8.8
		95	0.733	2.05×10^{-3}	0.9907	17	1.84×10^{-3}	0.9928	11.5

B

Sorbate	Sorbent	T (°C)	Diffusion pattern analysis			Full time analysis			Relative difference of D_{eff}/R_p^2, ε(%)[a]
			Slope	D_{eff}/R_p^2 (s^{-1})	R^2-value	L	D_{eff}/R_p^2 (s^{-1})	R^2-value	
Cumene	SSZ-42	120	1.715	8.84×10^{-5}	0.9810	35	7.15×10^{-5}	0.9825	23.6
		130	1.360	1.26×10^{-4}	0.9803	37	9.99×10^{-5}	0.9898	25.9
		140	1.031	1.87×10^{-4}	0.9901	40	1.51×10^{-4}	0.9902	24.0
		150	0.712	2.51×10^{-4}	0.9921	50	1.97×10^{-4}	0.9883	27.4
Toluene	SSZ-42	65	1.412	1.90×10^{-4}	0.9885	29	1.05×10^{-4}	0.9915	80.9
		80	1.082	4.02×10^{-4}	0.9937	26	2.11×10^{-4}	0.9908	90.5
		95	0.786	5.73×10^{-4}	0.9896	30	3.66×10^{-4}	0.9879	56.5

[a]In Tables 2–4, ε is calculated based on this expression: $\varepsilon = \left| \frac{D_{\text{eff}}/R_p^2(D_{\text{eff}}/l^2) \text{ from short time analysis} - D_{\text{eff}}/R_p^2(D_{\text{eff}}/l^2) \text{ from full time analysis}}{D_{\text{eff}}/R_p^2(D_{\text{eff}}/l^2) \text{ from full time analysis}} \right| \times 100\%$

Table 3 Summary of parameters from the ZLC analysis of cumene in SBA-16 and 1-methylnaphthalene in MCM-48 based on (A) three-dimensional model and (B) one-dimensional model

A

Sorbate	Sorbent	T (°C)	Diffusion pattern analysis			Full time analysis			Relative difference of D_{eff}/R_p^2, ε (%)
			Slope	D_{eff}/R_p^2 (s^{-1})	R^2-value	L	$D_{\text{eff}}R_p^2$ (s^{-1})	R^2-value	
Cumene	SBA-16	50	0.687	1.05×10^{-4}	0.9958	80	1.14×10^{-4}	0.9806	7.4
		70	0.614	1.32×10^{-4}	0.9973	80	1.41×10^{-4}	0.9927	6.5
		90	0.393	2.06×10^{-4}	0.9991	100	1.92×10^{-4}	0.9961	7.3
1-methylnaphthalene	MCM-48	50	2.628	2.35×10^{-4}	0.9980	14	2.56×10^{-4}	0.9917	8.1
		75	1.779	3.93×10^{-4}	0.9934	16	4.30×10^{-4}	0.9916	8.6
		100	1.117	6.37×10^{-4}	0.9983	20	6.93×10^{-4}	0.9979	7.9

B

Sorbate	Sorbent	T (°C)	Diffusion pattern analysis			Full time analysis			Relative difference of D_{eff}/l^2, ε(%)
			Slope	D_{eff}/l^2 (s^{-1})	R^2-value	L	D_{eff}/l^2 (s^{-1})	R^2-value	
Cumene	SBA-16	50	0.426	8.66×10^{-4}	0.8245	45	6.09×10^{-4}	0.9788	42.2
		70	0.373	1.13×10^{-3}	0.8025	45	7.57×10^{-4}	0.9876	49.4
		90	0.227	1.72×10^{-3}	0.7785	60	1.02×10^{-3}	0.9823	68.6
1-methylnaphthalene	MCM-48	100	0.521	9.71×10^{-3}	0.6726	11	3.94×10^{-3}	0.9893	146.5

Table 4 Summary of parameters from the ZLC analysis of heptane, cumene and mesitylene in SBA-15 samples based on (A) three-dimensional model and (B) one-dimensional model

A

Sorbate	Sorbent	T (°C)	Diffusion pattern analysis			Full time analysis			Relative difference of D_{eff}/R_p^2, ε (%)
			Slope	D_{eff}/R_p^2 (s^{-1})	R^2-value	L	D_{eff}/R_p^2 (s^{-1})	R^2-value	
Cumene	SBA-15-1	70	1.916	8.33×10^{-4}	0.9999	10	7.88×10^{-4}	0.9943	5.8
Heptane		10	1.983	6.12×10^{-4}	0.9998	12	6.25×10^{-4}	0.9985	2.0
		20	1.769	7.69×10^{-4}	0.9999	12	8.37×10^{-4}	0.9995	8.0
		30	1.410	1.06×10^{-3}	0.9997	12	1.10×10^{-3}	0.9983	3.8
Mesitylene	SBA-15-2	70	2.300	4.80×10^{-4}	0.9995	11	5.15×10^{-4}	0.9985	6.8
Cumene		50	2.045	6.65×10^{-4}	0.9995	11	6.99×10^{-4}	0.9945	4.8
		70	1.514	1.02×10^{-3}	0.9999	12	9.13×10^{-4}	0.9944	11.2
Heptane		20	1.407	1.22×10^{-3}	0.9997	12	1.15×10^{-3}	0.9980	5.8
		30	1.057	1.36×10^{-3}	0.9996	15	1.38×10^{-3}	0.9976	1.7
Heptane	SBA-15-3	10	1.275	1.36×10^{-3}	0.9995	12	1.39×10^{-3}	0.9565	2.1
		20	0.938	1.41×10^{-3}	0.9993	16	1.53×10^{-3}	0.9722	7.6
		30	0.690	1.67×10^{-3}	0.9997	20	1.66×10^{-3}	0.9936	0.7
Cumene		30	1.931	8.05×10^{-4}	0.9997	11	7.57×10^{-4}	0.9962	13.9
		50	1.445	9.61×10^{-4}	0.9987	13	8.52×10^{-4}	0.9922	12.8
		70	1.098	1.17×10^{-3}	0.9986	15	1.00×10^{-3}	0.9948	17.3
Mesitylene		30	2.883	3.83×10^{-4}	0.9993	10	3.86×10^{-4}	0.9942	0.8
		50	2.157	4.75×10^{-4}	0.9987	12	4.81×10^{-4}	0.9908	1.2
		70	1.671	5.82×10^{-4}	0.9982	14	5.83×10^{-4}	0.9913	0.2

B

Sorbate	Sorbent	T (°C)	Diffusion pattern analysis			Full time analysis			Relative difference of D_{eff}/l^2, ε(%)
			Slope	D_{eff}/l^2 (s^{-1})	R^2-value	L	D_{eff}/l^2 (s^{-1})	R^2-value	
Heptane	SBA-15-3	30	0.412	1.55×10^{-2}	0.8175	11	1.06×10^{-2}	0.9588	46.0

runs under various purging flow rates. The L values were generally found to be greater than 10, thus confirming a kinetically controlled process (Hufton and Ruthven 1993). The desorption curves were corrected with blank measurements to account for dead volumes**,** in which only two sintered discs, i.e., with no adsorbent present, were placed in the ZLC column.

4 Results and discussion

The ZLC results for heptane, cumene and mesitylene diffusion in SBA-15-1, SBA-15-2 and SBA-15-3 samples were reported elsewhere (Vinh-Thang et al. 2006). The experimental and theoretical ZLC response results for SBA-16, MCM-48 and SSZ-42 at different temperatures are compared in Figs. 1 and 2. The three-dimensional full time model was applied to fit experimental ZLC curves of SBA-16 and MCM-48 samples, while the one-dimensional full time model was applied to fit SSZ-42 data. Clearly, good agreements between experimental results and theoretical fittings were observed. The extracted diffusion time constants and L values for all samples are summarized in Tables 2(A), 3(A) and 4(A). L values are all greater than 10, indicating that desorption is kinetically controlled, and analysis of the diffusion pattern from ZLC desorption curves can be accomplished according to the theoretical criteria, as discussed in the theory section. The experimental ZLC data for SBA-15, SBA-16 and MCM-48 were also fitted by the one-dimensional full time model, and SSZ-42 data were fitted by the three-dimensional full time model. The regression coefficients (R^2-values), which represent how well the model fits the experimental data, are included in Tables 2–4. Apparently, both one- and three-dimensional, full tim**e,** solution models provide a reasonable fit of all experimental ZLC data, e.g., R^2-values larger than 0.95, thus confirming the inadequacy of the full time solution model being used alone to differentiate between one- and three-dimensional diffusion patterns.

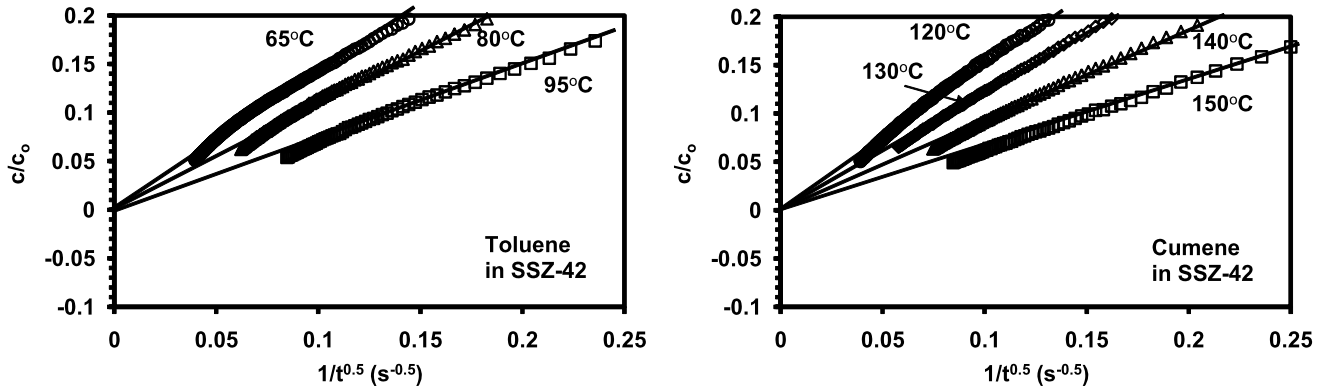

Fig. 3 Dimensional diffusion analysis of toluene and cumene in SSZ-42 sample at different temperatures

The analysis of the diffusion pattern was firstly conducted on the microporous SSZ-42, which is a representative of an undulating one-dimensional, 12-membered-ring channel system (Sarshar et al. 2009). The plots based on diffusion pattern analysis, i.e., c/c_0 versus $1/\sqrt{t}$ for SSZ-42 are displayed in Fig. 3. The zero intercept reveals that the diffusion of toluene and cumene in SSZ-42 complies with one-dimensional diffusion pattern, corresponding to one-dimensional structure. The diffusion patterns were found independent of the measurement temperature and the nature of sorbate molecules, thus confirming sufficiency of the analysis based on the diffusion pattern model.

The method was further applied in investigating the diffusion pathways of mesoporous SBA-15, SBA-16 and MCM-48 silicas. The plots based on diffusion path analysis are represented in Figs. 4 and 5. All plots exhibit the negative intercepts corresponding to the values of $-1/L$ regardless of measurement temperatures and probe molecules, thus being consistent with the three-dimensional diffusion path, i.e., spherical model. These results are expected for MCM-48 and SBA-16 samples, since MCM-48 is known to have a well-defined three-dimensional network structure of cylindrical pores, while SBA-16 has a cage-like mesoporous structure with a three-dimensional cubic body-centered symmetry. Three SBA-15 samples have small amounts of micropore volume as shown in Table 1. It has been reported that the porous structure of SBA-15 consists not only of two-dimensional large, uniform, and highly ordered channels, but also contains much smaller complementary pores within walls of main channels (Ryoo et al. 2000; Vinh-Thang et al. 2005b). These intrawall pores have a wide range of sizes including both micropores and smaller mesopores, and they provide a connection between large mesopores of the main channels, rendering the three-dimensional diffusion behavior of the SBA-15 samples.

As suggested in the theory section, further analysis is required to be carried out to verify the conclusions regarding the diffusion paths of various samples. The diffusion time constants (D_{eff}/R_p^2) or (D_{eff}/l^2) for all samples determined from both the diffusion path analysis and the full time method, and their relative differences are summarized in Tables 2–4. Tables 2(A), 3(A) and 4(A) indicate that the differences of diffusion time constants are relatively small ranging from 0.4–17.3%, when the three-dimensional model was applied to the SBA-15, SBA-16 and MCM-48 data, and the one-dimensional model to the SSZ-42 data. However, when the one-dimensional model was applied to the SBA-15, SBA-16 and MCM-48 data and the three-dimensional model to the SSZ-42 data, the relative differences of diffusion time constants, shown in Tables 2(B), 3(B) and 4(B), become much larger, ranging from 23.6–146.5%. This demonstrates that, if the model exactly represents the diffusion path of the samples, the obtained diffusion time constants derived from both methods exhibit reasonable agreements. Otherwise, they show significant deviations. This analysis indirectly supports that the three-dimensional model exactly represents the diffusion path of SBA-15, SBA-16 and MCM-48, and one-dimensional model represents the diffusion path of SSZ-42. In addition, the R^2-values obtained from the diffusion path analysis, using correct models (Tables 2(A), 3(A) and 4(A)) are generally superior to those obtained from inappropriate models (Tables 2(B), 3(B) and 4(B)). This provides further evidence regarding use of an appropriate model to fit experimental data.

It can be observed from Table 2 that all R^2-values from either one- or three-dimensional diffusion path analysis for SSZ-42 data are greater than 0.98, indicating the good fittings. There exist minor deviations from linearity for SSZ-42 shown in Fig. 3, which could be ascribed to the uncertainty of measurements in the short time region (Cavalcante et al. 1997), resulting in errors in data analysis. Therefore, it is important to check the consistence of extracted diffusion parameters from both diffusion path analysis and full time analysis.

In contrast to the microscopic techniques of diffusion measurement which may provide direct evidence on the di-

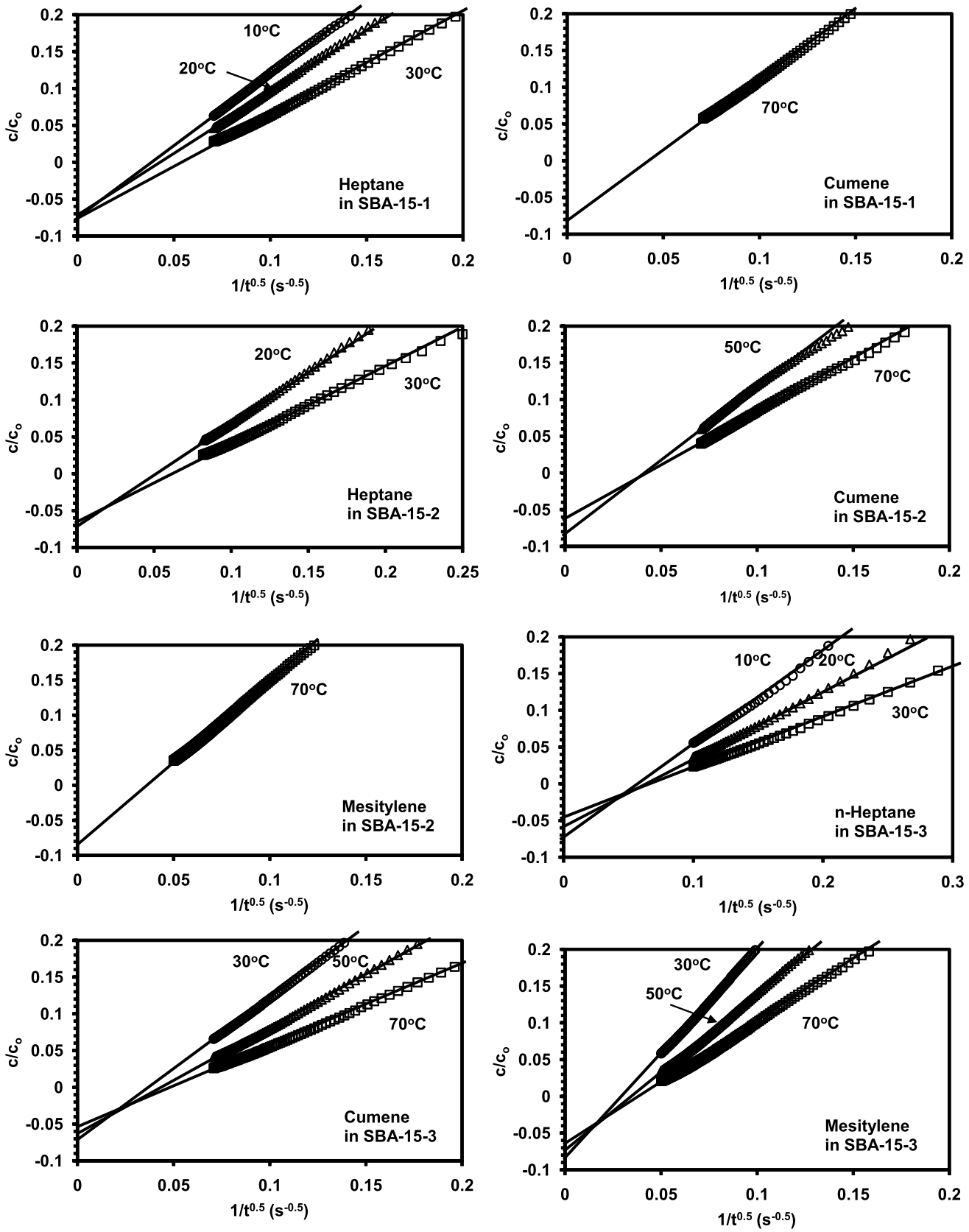

Fig. 4 Dimensional diffusion analysis of heptane, cumene and mesitylene in SBA-15-1, SBA-15-2 and SBA-15-3 samples at different temperatures

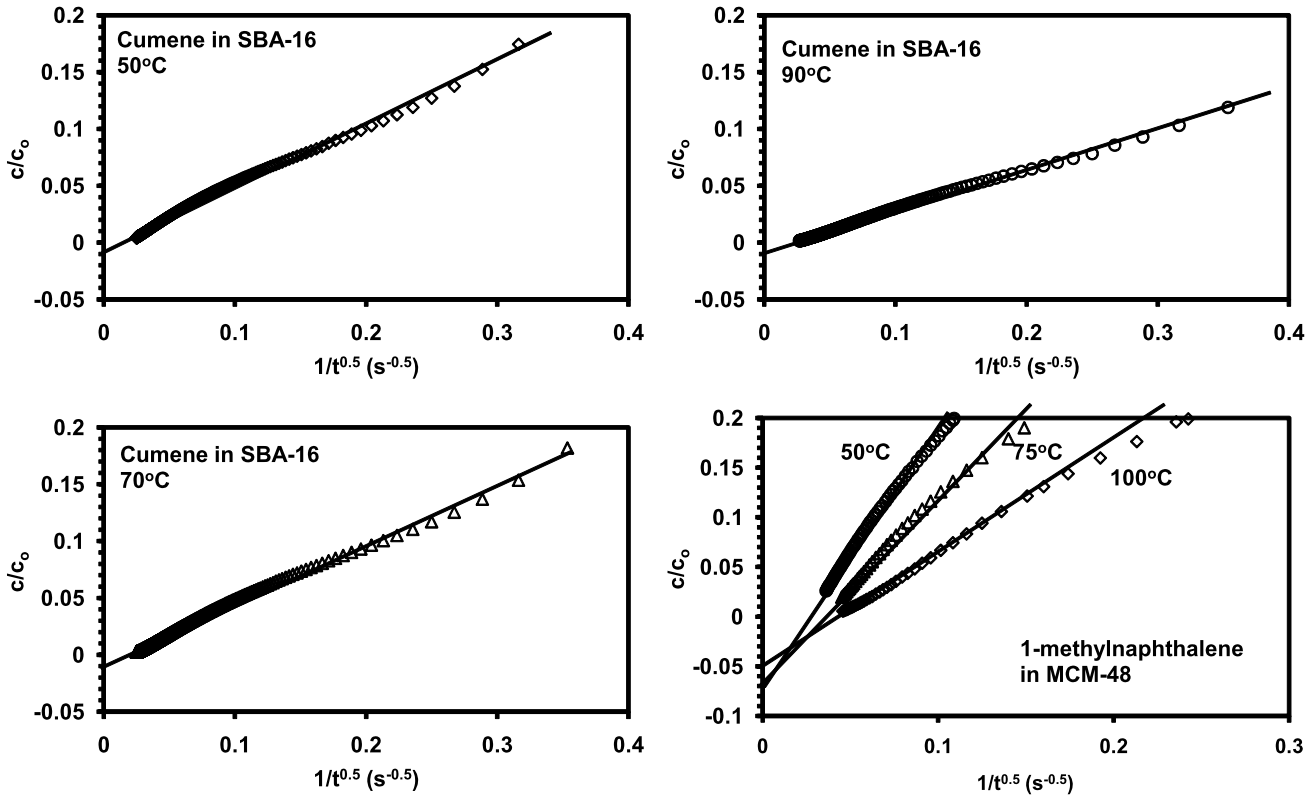

Fig. 5 Dimensional diffusion analysis of cumene in SBA-16, and 1-methylnaphthalene in MCM-48 at different temperatures

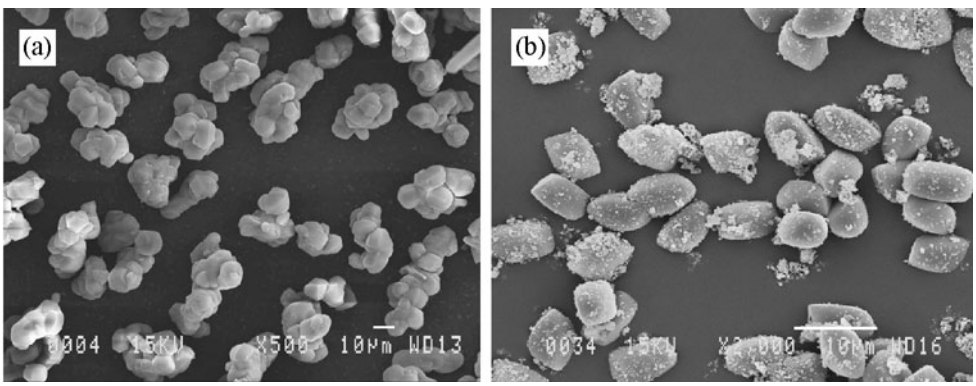

Fig. 6 SEM images of (**a**) SBA-15-2 (Vinh-Thang et al. 2005b), and (**b**) SSZ-42 (Sarshar et al. 2009)

rection of molecular propagation and, hence, on the dimensionality of the observed diffusion phenomena, macroscopic diffusion measurements have to be based on model considerations. In the ZLC case, as mentioned in the theory section, it is the difference in the time dependence over the last period of desorption, namely for $c/c_0 < 0.2$. Apart from the evidence of mathematical analysis, this result may also be anticipated by rationalizing the differences in matter release from a one-dimensional body in comparison with a three-dimensional body. This means, however, that, with respect to their transport properties, the particles under study may in fact be considered as such "bodies", i.e., as quasi-single crystals, rather than as polycrystalline materials. The scanning electron microscopy (SEM) images of representative SBA-15-2 and SSZ-42 (Fig. 6) reveal that their "bodies" are different, where the former exhibits a three-dimensional property, while the latter one a one-dimensional property.

5 Conclusions

The diffusion patterns of mesoporous SBA-15, SBA-16, MCM-48 silicas and microporous SSZ-42 sample were characterized from ZLC desorption curves using a simple analysis. According to that analysis the diffusion path in SBA-15, SBA-16, MCM-48 samples was found to be three-

dimensional, while it was found one-dimensional in SSZ-42. The diffusion path patterns did not vary with temperature or nature of sorbate molecules, thus further confirming adequacy of the proposed analysis. The intrawall pores in the mesoporous framework account for the three-dimensional diffusion system of SBA-15 samples.

This method of diffusion path analysis is confirmed to be an effective method for fast and relatively inexpensive characterization of microporous and mesoporous materials. It can be used alone or as a supplement to the conventional methods, e.g., TEM analysis, in performing a more comprehensive analysis of materials with unknown pore structures.

Acknowledgements We gratefully acknowledge important contributions made by Dr. Ling Huang, Dr. Hoang Vinh-Thang, Oliver C. Gobin and Zahra Sarshar by taking a part in the synthesis and characterizations of materials used in this study. Financial support by NSERC is also acknowledged.

References

Brandani, S., Ruthven, D.M.: Analysis of ZLC desorption curves for gaseous systems. Adsorption **2**, 133 (1996)

Cavalcante, C.L., Brandani, S., Ruthven, D.M.: Evaluation of the main diffusion path in zeolites from ZLC desorption curves. Zeolites **18**, 282 (1997)

Doadrio, J.C., Sousa, E.M.B., Izquierdo-Barba, I., Doadrio, A.L., Perez-Pariente, J., Vallet-Regi, M.: Functionalization of mesoporous materials with long alkyl chains as a strategy for controlling drug delivery pattern. J. Mater. Chem. **16**, 462 (2006)

Eić, M., Ruthven, D.M.: A new experimental-technique for measurement of intracrystalline diffusivity. Zeolites **8**, 40 (1988)

Gobin, O.C., Wan, Y., Zhao, D.Y., Kleitz, F., Kaliaguine, S.: Mesostructured silica SBA-16 with tailored intrawall porosity, part 1: synthesis and characterization. J. Phys. Chem. C **111**, 3053 (2007)

Huang, L., Huang, Q.L., Xiao, H.N., Eic, M.: Al-MCM-48 as a potential hydrotreating catalyst support, II: diffusion property study. Microporous Mesoporous Mater. **114**, 121 (2008)

Hufton, J.R., Ruthven, D.M.: Diffusion of light alkanes in silicalite studied by the zero length column method. Ind. Eng. Chem. Res. **32**, 2379 (1993)

Iliyas, A., Zahedi-Niaki, M.H., Eic, M., Kaliaguine, S.: Control of hydrocarbon cold-start emissions: a search for potential adsorbents. Microporous Mesoporous Mater. **102**, 171 (2007)

Kresge, C.T., Leonowicz, M.E., Roth, W.J., Vartuli, J.C., Beck, J.S.: Ordered mesoporous molecular-sieves synthesized by a liquid-crystal template mechanism. Nature **359**, 710 (1992)

Liu, A.M., Hidajat, K., Kawi, S., Zhao, D.Y.: A new class of hybrid mesoporous materials with functionalized organic monolayers for selective adsorption of heavy metal ions. Chem. Commun., 1145 (2000)

Malekian, A., Vinh-Thang, H., Huang, Q.L., Eić, M., Kaliaguine, S.: Evaluation of the main diffusion path in novel micro-mesoporous zeolitic materials with the Zero Length Column method. Ind. Eng. Chem. Res. **46**, 5067 (2007)

Newalkar, B.L., Choudary, N.V., Kumar, P., Komarneni, S., Bhat, T.S.G.: Exploring the potential of mesoporous silica, SBA-15, as an adsorbent for light hydrocarbon separation. Chem. Mater. **14**, 304 (2002)

Rioux, R.M., Song, H., Hoefelmeyer, J.D., Yang, P., Somorjai, G.A.: High-surface-area catalyst design: synthesis, characterization, and reaction studies of platinum nanoparticles in mesoporous SBA-15 silica. J. Phys. Chem. B **109**, 2192 (2005)

Ryoo, R., Ko, C.H., Kruk, M., Antochshuk, V., Jaroniec, M.: Block-copolymer-templated ordered mesoporous silica: array of uniform mesopores of mesopore-micropore network? J. Phys. Chem. B **104**, 11465 (2000)

Sarshar, Z., Zahedi-Niaki, M.H., Huang, Q.L., Kaliaguine, S.: Synthesis, structural and acidity characterizations of the large-pore zeolite SSZ-42 for controlling cold-start emissions. Microporous Mesoporous Mater. **118**, 373 (2009)

Serrano, D.P., Galleja, G., Botas, J.A., Gutierrez, F.J.: Adsorption and hydrophobic properties of mesostructured MCM-41 and SBA-15 materials for volatile organic compound removal. Ind. Eng. Chem. Res. **43**, 7010 (2004)

Trong-On, D., Desplantier-Giscard, D., Danumah, C., Kaliaguine, S.: Perspectives in catalytic applications of mesostructured materials. Appl. Catal. A, Gen. **253**, 545 (2003)

Vinh-Thang, H., Huang, Q.L., Eić, M., Trong-On, D., Kaliaguine, S.: Adsorption of C_7 hydrocarbons on biporous SBA-15 mesoporous silica. Langmuir **21**, 5094 (2005a)

Vinh-Thang, H., Huang, Q.L., Eić, M., Trong-On, D., Kaliaguine, S.: Structure and diffusion characterization of SBA-15 materials. Langmuir **21**, 2051 (2005b)

Vinh-Thang, H., Huang, Q.L., Eić, M., Trong-On, D., Kaliaguine, S.: Effect of the intrawall microporosity on the diffusion characterization of bi-porous SBA-15 materials. Stud. Surf. Sci. Catal. **149**, 591 (2006)

Xu, X., Song, C., Andresen, J.M., Miller, B.G., Scaroni, A.W.: Preparation and characterization of novel CO_2 "molecular basket" adsorbents based on polymer-modified mesoporous molecular sieve MCM-41. Microporous Mesoporous Mater. **62**, 29 (2003)

Zhao, D.Y., Huo, Q., Feng, J., Chmelka, B.F., Stucky, G.D.: Nonionic triblock and star diblock copolymer and oligomeric surfactant syntheses of highly ordered, hydrothermally stable, mesopoours silica structures. J. Am. Chem. Soc. **120**, 6024 (1998)

Zhao, J.W., Gao, F., Fu, Y., Wan, J., Yang, P., Zhao, D.Y.: Biomolecule separation using large pore mesoporous SBA-15 as a substrate in high performance liquid chromatography. Chem. Commun. 752, (2002)